Core excitations of naphthalene: Vibrational structure versus chemical shifts

I. Minkov and F. Gel'mukhanov[a)]
Theoretical Chemistry, Roslagstullsbacken 15, Royal Institute of Technology, S-106 91 Stockholm, Sweden

R. Friedlein, W. Osikowicz, and C. Suess
Department of Physics, Linköping University, IFM S-581 83 Linköping, Sweden

G. Öhrwall
Department of Physics, Uppsala University, P.O. Box 530, S-751 21 Uppsala, Sweden

S. L. Sorensen
Department of Synchrotron Radiation Research, Institut of Physics, Lund University, P.O. Box 118, S-221 00 Lund, Sweden

S. Braun,[b)] R. Murdey, and W. R. Salaneck
Department of Physics, Linköping University, IFM S-581 83 Linköping, Sweden

H. Ågren
Theoretical Chemistry, Roslagstullsbacken 15, Royal Institute of Technology, S-106 91 Stockholm, Sweden

(Received 4 May 2004; accepted 28 June 2004)

High-resolution x-ray photoelectron emission (XPS) and near-edge x-ray absorption fine structure (NEXAFS) spectra of naphthalene are analyzed in terms of the initial state chemical shifts and the vibrational fine structure of the excitations. Carbon atoms located at peripheral sites experience only a small chemical shift and exhibit rather similar charge-vibrational coupling, while the atoms in the bridging positions differ substantially. In the XPS spectra, C-H stretching modes provide important contributions to the overall shape of the spectrum. In contrast, the NEXAFS spectrum contains only vibrational progressions from particular C-C stretching modes. The accuracy of *ab initio* calculations of absolute electronic transition energies is discussed in the context of minute chemical shifts, the vibrational fine structure, and the state multiplicity. © *2004 American Institute of Physics.* [DOI: 10.1063/1.1784450]

I. INTRODUCTION

In recent years, significant technological advances allow the production of highly monochromatic, polarized x-ray synchrotron radiation with a spectral resolving power of the order of 10^4. High experimental resolution is the key to observe vibrational fine structure and minute initial state chemical shifts in free molecules[1–4] and possibly even in adsorbates.[5,6] The high resolution may even reveal ''hidden'' processes, in particular, the nuclear dynamics connected with ionization processes,[7–10] electronic excitations,[11–13] or possibly even effects associated with charge transport at interfaces[6,14] and in solids[12,13,15,16] might be studied. The energy separation between core-electronic states on different sites,[17,18] and the existence of selection rules for transitions to unoccupied valence orbitals,[19,20] make core excitations particularly useful for the study of partial or local charge and vibrational density distributions in small and medium-size molecules,[18] and of the geometrical relaxation associated with the presence of charges.[21] Different valence electron densities at the various atomic sites give rise to differences in the total energies of excitations, usually called ''initial state chemical shifts'' of core levels.[22] Shifts of a fraction of an eV are sufficient to produce distinguishable lines in the spectra.

The dynamics of nuclear relaxation processes can in some cases be resolved thanks to the high-energy resolution. Recent advances in experimental techniques call for a better understanding of the underlying physical processes by simulations of x-ray spectra with refined theoretical models. The study of processes in medium-size molecules like naphthalene (Fig. 1) might provide an understanding of even more complex systems, larger molecules, and even solids.

In a system with two or more equivalent atoms, photoionization or core excitation gives rise to several almost degenerate electronic transitions. It is well known[23] that such quasidegenerate excited states interact with each other via nontotally symmetric vibrational modes. This results in the localization of core holes. In the case of nonequivalent atoms of the same chemical element, on the other hand, the quasidegeneracy of the core-excited states is lifted. An accurate calculation of electronic and vibrational energies is therefore crucial to reveal the nature of interactions between a charge or an excitation and the coupled nuclear-electronic system of the molecule.

In the present paper we report high-resolution C(1*s*) photoionionization and x-ray absorption spectra of the free naphthalene molecule followed by their interpretation in

[a)]Permanent address: Institute of Automation and Electrometry, 630090 Novosibirsk, Russia.
[b)]Formerly S. Marciniak.

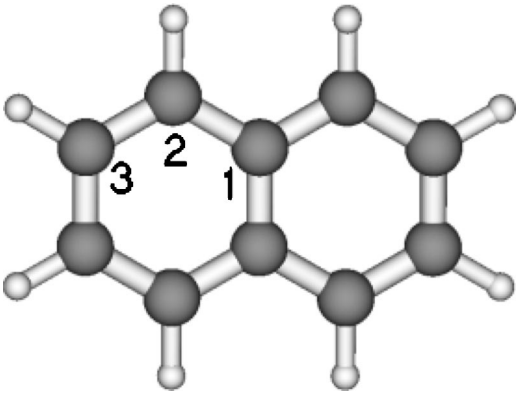

FIG. 1. The naphthalene molecule and its chemically different atomic sites.

terms of electronic and vibronic relaxation mechanisms. In particular, the relation between excitations at chemically shifted atomic sites and their coupling to molecular vibrations is discussed.

II. EXPERIMENT

The gas-phase spectra were obtained at beamline I411 at MAX-Lab in Lund, Sweden.[24] A gas cell with an external feed was used allowing high local gas densities (local pressure $>1\times10^{-5}$ mbar) and moderate temperatures of 40 ±20 °C in the target zone.

The Scienta SES-200 photoelectron spectrometer was turned to the ''magic angle'' (54.7°) between the electric field vector of the light and the direction of the electron emission. The near-edge x-ray absorption fine structure (NEXAFS) spectrum was recorded in 5 meV photon energy steps with the Auger yield technique. The C KLL Auger electrons were collected with a kinetic-energy window between 240 and 274 eV. The intensity was normalized by the incoming photon flux as measured using the current from a gold grid. For energies at the $C(1s)$ absorption edge, a photon energy resolution of 50–60 meV was employed. For the x-ray photoelectron spectroscopy (XPS) measurements, the spectral width of the incident radiation was matched with the energy resolution of the analyzer. The total energy resolution for the $C(1s)$ XPS line measured with 350 eV photons is estimated to be about 75 meV.

Each scan was saved separately to minimize the effects of beam instabilities during the measurements. During normal, stable operation, drifts at the MAX-II storage ring are typically <1 meV/min. The photon energies and the kinetic energies of the electrons were calibrated from the position of the $Ar(2p)$ line excited by first and second-order light. Absolute photon and electron energies have an uncertainty of about 100 meV.

III. THEORY

Our calculations are based on the linear coupling model—the excited state potential energy surface (PS) E_{exc} is approximated by a displaced ground state harmonic potential surface. While the minimum of the excited state PS might be displaced from that of the ground state, a similar curvature is assumed to be present. In spite of its simplicity, this model is known to be of good accuracy for a number of cases.[25,26] Using harmonic approximation, the Hamiltonian has the following form (atomic units):

$$\hat{H}=\sum_{\alpha}\left(-\frac{\partial^2}{\partial Q_{\alpha}^2}+\frac{1}{2}\omega_{\alpha}^2 Q_{\alpha}^2\right), \tag{1}$$

where Q_{α} and ω_{α} are the normal coordinates and the frequencies of the vibrational mode α. The displacement d_{α} of each normal mode's excited state PS from the ground state geometry is connected to the gradient of the PS

$$d_{\alpha}=\frac{G_{\alpha}}{\omega_{\alpha}^2},\quad G_{\alpha}=\frac{\partial E_{\mathrm{exc}}}{\partial Q_{\alpha}}. \tag{2}$$

In order to obtain the probability for excitation from the ground state vibrational level 0 to a vibrational level n_{α} for a particular mode α, the overlap integral between the two vibronic wave functions [the Franck-Condon (FC) amplitude][23] is needed,

$$\langle 0|n_{\alpha}\rangle=(-1)^{n_{\alpha}}e^{-(x/2)}\frac{x^{(n_{\alpha}/2)}}{\sqrt{n_{\alpha}!}}. \tag{3}$$

Here $x=\omega_{\alpha}d_{\alpha}^2/2=G_{\alpha}^2/2\omega_{\alpha}^3$ is a dimensionless parameter, which depends on the excited state PS gradient G_{α}.

The total overlap integral is a product of contributions of all individual modes

$$\langle 0|n\rangle=\prod_{\alpha}\langle 0|n_{\alpha}\rangle. \tag{4}$$

It should be noted that the excited state PS gradient and FC amplitude (3) could differ for the ionization and the excitation processes. The reason for this can be easily understood in terms of the Koopmans' theorem,

$$G_{\alpha}^{\mathrm{ion}}=\frac{\partial}{\partial Q_{\alpha}}[E(1s^{-1})-E_0]\approx-\frac{\partial}{\partial Q_{\alpha}}\epsilon_{1s},$$

$$G_{\alpha}^{\mathrm{exc}}=\frac{\partial}{\partial Q_{\alpha}}[E(1s\rightarrow\nu)-E_0]\approx-\frac{\partial}{\partial Q_{\alpha}}(\epsilon_{\nu}-\epsilon_{1s}),$$

where ϵ_{1s} and ϵ_{ν} are the orbital energies of the $1s$ and the νth orbital. Comparison of these gradients shows that the vibrational structure of NEXAFS and XPS spectra is different because of the $(\partial\epsilon_{\nu}/\partial Q_{\alpha})$ term. Notice that in our simulations we calculated the gradients strictly, without using the Koopmans' approximation.

The x-ray absorption cross section was calculated in the Born-Oppenheimer approximation

$$\sigma_{\mathrm{abs}}(\omega)\propto\sum_{e,n}\frac{f_{0e}\langle 0|n\rangle^2}{[\omega-(E_e-E_0)-(\epsilon_n^e-\epsilon_0)]^2+\Gamma^2}, \tag{5}$$

where ω is the photon frequency; f_{0e} is the oscillator strength of the electronic transition $0\rightarrow e$; E_e, ϵ_n^e, and E_0, ϵ_0 are the excited and ground state electronic and vibrational energies, respectively; $\langle 0|n\rangle^2$ is the FC factor.

The cross section of the core-ionization process reads

$$\sigma_{\mathrm{XPS}}(E) \propto \sum_{N,n} \frac{D_N^2(E)\langle 0|n\rangle^2}{[BE - I_N - (\epsilon_n^e - \epsilon_0)]^2 + \Gamma^2}. \quad (6)$$

Here $BE = \omega - E$, is the energy of the photoelectron on a binding energy scale, E the kinetic energy of the photoelectron, and I_N the C$(1s)$ binding energy of the Nth carbon atom. In the simulations the square of the transition dipole moments of the photoionization process, $D_N^2(E)$, is assumed to be equal for all atoms. This approximation holds only for large photoelectron energies.

Calculation of both core excitation and ionization are performed using the independent channel approximation.[27] This approximation is valid because of the large energy and spatial separation of core orbitals of different atoms. This approach has previously been tested and justified to be of good accuracy.[28–30]

IV. COMPUTATION

The geometry of the molecule has been optimized with the GAUSSIAN 03 package[31] at the B3LYP/6-311G** level. The vibrational analysis has been done at a [10,10]-CASSCF level of theory, with the same 6-311G** basis set using the DALTON program package.[32] All transition dipole moments and excitation energies were calculated using a modified version of the DEMON code[33] employing the ΔDFT (DFT—density functional theory) method. Two different nonlocal density functionals were tested: BP86 and PBE (for both exchange and correlation energy). In order to account for core-hole relaxation, we have made use of a double-basis technique.[34] For all carbon atoms, except the one undergoing core excitation, an effective core-potential basis set of good quality was used. In order to properly describe changes in the electronic structure of the excited atomic center, the region in its vicinity is described by a much larger, diffuse IGLO-III basis set. Structural relaxation could be responsible for breaking or lowering the symmetry of the core-excited system.[1,3] Therefore, no symmetry was preassumed in any part of the core-hole calculation.

In all of the mentioned codes there is no implemented procedure for an analytical derivation of excited state energy gradients. Therefore, the gradients (2) needed for obtaining FC factors have been calculated by a numerical differentiation of the excited state PS. For each mode, three points of the PS were calculated: one at the ground state geometry and two symmetrically displaced in positive and negative directions ($Q_\alpha = 0, \pm 7.26$ a.u. $\sqrt{\text{amu}}$). The centered derivative of these three points was taken.

The displaced geometries were generated using the following transformation:

$$X_{\mathrm{im}} = X_{0m} + A_{\mathrm{im},\alpha} \frac{Q_\alpha}{\sqrt{1822}},$$

where X_{im} is the displaced Cartesian coordinate i of the atom m (in a.u.), X_{0m} is the ground state Cartesian coordinate, Q_α is the normal coordinate of the normal vibrational mode α (in a.u. $\sqrt{\text{amu}}$); $A_{\mathrm{im},\alpha}$ is a matrix transforming the normal to Cartesian coordinates.

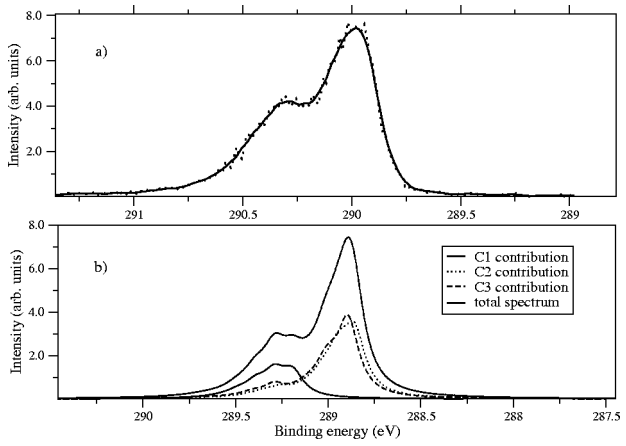

FIG. 2. Experimental (a) and calculated (b) C$(1s)$ photoelectron spectrum of naphthalene.

Two different values for the life-time vibrational broadening have been chosen to account for the different spectral resolution achieved in the NEXAFS and XPS experiments. The half width at half maximum is $\Gamma = 45$ meV for the NEXAFS simulations, while $\Gamma = 70$ meV for XPS. For each set of spectra, Γ is assumed to be the same for all transitions.

V. RESULTS AND DISCUSSION

A. XPS

In Fig. 2 the experimental and simulated C$(1s)$ photoelectron spectra are presented [Figs. 2(a) and 2(b), respectively]. The calculated vertical binding energies of the C$(1s)$ electrons at the three distinguishable carbon atom sites of the naphthalene molecule (denoted C1, C2, and C3 in Fig. 1) are listed in Table I. These values are about 1 eV lower than those obtained experimentally. Such a difference is expected in the framework of the ΔDFT method.[27] It was also found that the results produced by the PBE and BP86 functionals differ insignificantly.

Clearly, the shapes of the experimental and theoretical spectra match quite well allowing an assignment of the individual spectral features (Fig. 3). The spectrum does not exhibit any resolved vibrational fine structure. Nevertheless, vibrational degrees of freedom determine the width and the shape of the individual C1, C2, and C3 lines forming the overall profile [see Figs. 2(b) and 3].

The intense peak at the low-binding-energy side arises from a superposition of spectral weight for the C2 and C3 atomic sites. The chemical shift between these sites is quite small,[28] about 25 meV. The profiles of the two contributions are almost identical, which indicates that the photohole couples to similar vibrational modes on both atomic sites. The main contribution comes from coupling to C-C stretch-

TABLE I. Vertical C$(1s)$ binding energies for the three symmetrically distinguishable carbon atoms in naphthalene.

	C1	C2	C3
I_N (eV)	289.303	288.965	288.988

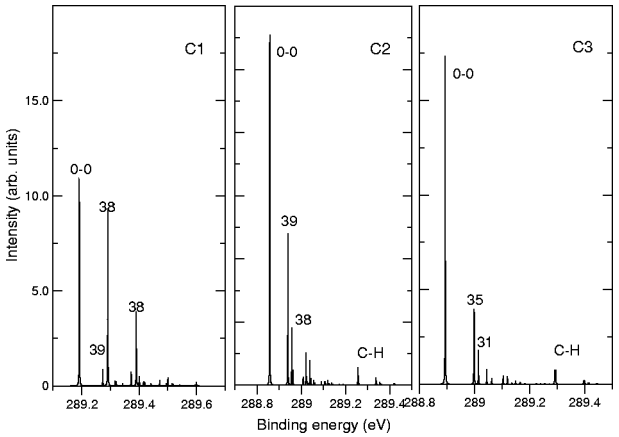

FIG. 3. Spectral lines of the vibrationally resolved XPS for the three atomic sites, without life-time broadening. Numbers indicate the particular vibrational mode which is excited.

ing modes and only minor excitations of C-H stretching. However, the region of the C-C stretching modes is dominated by only one of them (Fig. 3 and Tables II, III, and IV). Since many modes are involved, a clear vibrational splitting cannot be observed.

C-H vibrational contributions are absent for the C1 site which is not connected to hydrogen atoms. Since fewer modes are involved at C1, the profile also appears slightly more structured and does not have a pronounced tail like those of the two other sites. The binding energy for the C1 site is about 0.3 eV higher than that of the C2 and C3 sites. The C1 peak overlaps with the long tails of the C2 and C3 atoms leading to a plateau in the total spectrum.

It is instructive to compare the coupling between core holes and vibrations to the charge-vibrational coupling for valence holes in naphthalene. The ionization of the highest occupied molecular orbital (HOMO) exhibits a pronounced high frequency progression of about 180 meV, which is attributed to the superposition of two unresolved, totally symmetric C-C stretching modes of 170.4 and 196.8 meV interacting nonadiabatically, and small contributions of C-H out-of-plane bending modes of about 60 meV.[10] A strong increase of the coupling to such low-frequency vibrations is observed for ionization of valence states at higher binding energy, e.g., of the HOMO-1 and HOMO-2.[10]

A strong dependence of the charge-vibrational coupling on the orbitals involved is confirmed by the present results for core ionization. While low-energetic C-H out-of-plane bending modes are dominant for some valence levels, such as for the HOMO-2, they are virtually absent in the case of core ionization. Additionally, the dominance of a single C-C stretching mode for the C(1*s*) ionization does not match the behavior for any of the valence orbitals and might also not be expected since the creation of a core hole breaks the high symmetry of the molecule.[1,3]

TABLE II. Franck-Condon factors for the strongest vibrational modes C(1*s*) photoionization at the C1 site—XPS.

			FC factors		
Mode	ω (eV)	Symmetry	$\langle 0\|0\rangle^2$	$\langle 0\|1\rangle^2$	$\langle 0\|2\rangle^2$
11	0.210	A_g	0.954	0.044	0.001
12	0.205	B_{3u}	0.988	0.012	0.000
23	0.151	B_{2u}	0.989	0.011	0.000
28	0.129	B_{3u}	0.979	0.021	0.000
30	0.125	B_{3u}	0.974	0.025	0.000
38	0.099	A_g	0.426	0.363	0.155
39	0.082	A_u	0.923	0.073	0.003

TABLE III. Franck-Condon factors for the strongest vibrational modes C(1*s*) photoionization at the C2 site—XPS.

			FC factors		
Mode	ω (eV)	Symmetry	$\langle 0\|0\rangle^2$	$\langle 0\|1\rangle^2$	$\langle 0\|2\rangle^2$
17	0.170	A_g	0.989	0.010	0.000
19	0.167	B_{1g}	0.977	0.022	0.000
23	0.151	B_{2u}	0.976	0.024	0.000
35	0.105	B_{2g}	0.958	0.041	0.001
38	0.099	A_g	0.850	0.139	0.011
39	0.082	A_u	0.649	0.281	0.061

B. NEXAFS

The measured C(1*s*) NEXAFS spectrum in the region of the x-ray absorption threshold and in a wider photon energy range (inset) is shown in Fig. 4. There is only a weak resemblance to an earlier spectrum from condensed naphthalene films.[35] The originally dominating π^* resonance has theoretically been described[28] to be actually composed of two resonances. These resonances are now clearly resolved. The first resonance denoted π_1^* occurs between $\hbar\omega$=284.7 and 285.4 eV; the second denoted π_2^* between $\hbar\omega$=285.6 and 286.5 eV. Additional resonances denoted 3, 4, 5, and σ_6^* with contributions from either π^* or σ^* symmetry[28] have their maxima at about $\hbar\omega$=287.3, 288.5, 290.2, and 293.8 eV.

In the present highly resolved spectrum, the π_1^* resonance exhibits even a very pronounced fine structure with individual peaks split by about 170 meV. Such a progression is characteristic for C-C stretching modes. For a relatively large molecule like naphthalene, the presence of this clearly resolved vibrational fine structure is remarkable, since it requires confinement of excitations to only one atomic site, or, in case of two or more sites that the chemical shift between them coincides (accidently) with the vibrational energy of about 170 eV. Furthermore, the sharpness of the peaks (with a width of the order of 160 meV) points to a rather selective

TABLE IV. Franck-Condon factors for the strongest vibrational modes C(1*s*) photoionization at the C3 site—XPS.

			FC factors		
Mode	ω (eV)	Symmetry	$\langle 0\|0\rangle^2$	$\langle 0\|1\rangle^2$	$\langle 0\|2\rangle^2$
18	0.169	B_{2u}	0.982	0.018	0.000
23	0.151	B_{2u}	0.956	0.043	0.001
31	0.121	B_{1g}	0.901	0.093	0.005
35	0.105	B_{2g}	0.798	0.180	0.020
36	0.104	B_{3g}	0.952	0.046	0.001

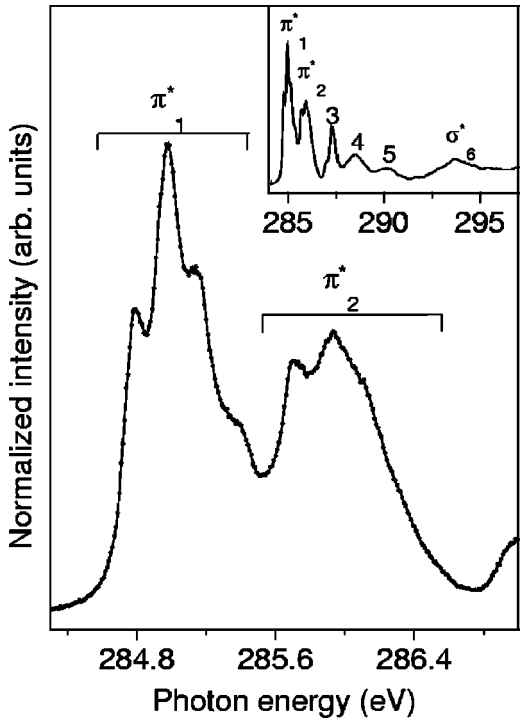

FIG. 4. Experimental NEXAFS spectrum of naphthalene in a wider and narrower (inset) energy range. Individual resonances are marked as π_1^*, π_2^*, 3, 4, 5, and σ_6^*.

coupling to vibrations in the core-excited state. These experimental observations represent a challenge to the present accuracy of the theoretical treatment of electronic energies (of the order of a few 10 meV for photon energies of about 285 eV) and the vibrational coupling in core-excited states.

The first two NEXAFS resonances π_1^* and π_2^* contain predominantly transitions from the 1*s* level to the lowest unoccupied molecular orbital (LUMO).[28] Feature π_1^* comprises overlapping contributions from vibrationally broadened C2 and C3 excitations (see Figs. 4 and 5). The C2 contributions are slightly lower in energy and cover a wider energy range than those from the C3 site. The C1 peak is

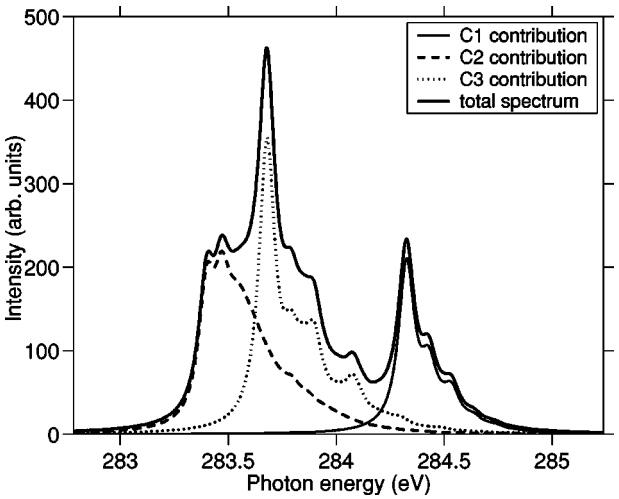

FIG. 5. Calculated NEXAFS spectrum of naphthalene and the contributions from the three chemically different atomic sites.

TABLE V. Franck-Condon factors for the strongest vibrational modes in the core excitation at the C1 site—NEXAFS.

			FC factors		
Mode	ω (eV)	Symmetry	$\langle 0\|0\rangle^2$	$\langle 0\|1\rangle^2$	$\langle 0\|2\rangle^2$
10	0.214	B_{2u}	0.984	0.016	0.000
11	0.210	A_g	0.888	0.105	0.006
19	0.167	B_{1g}	0.964	0.035	0.001
35	0.105	B_{2g}	0.817	0.165	0.017
38	0.099	A_g	0.879	0.113	0.007

positioned at higher energy, as expected from the core-level binding energies, and gives rise to the π_2^* feature. Our calculations show that core excitations into the LUMO at the C1 site display a pronounced vibrational structure caused by one particular mode (Table V). This fine structure is not visible in the experimental spectrum. Instead, the π_2^* resonance has a double structure (Fig. 4). One possible explanation for this discrepancy could be the presence of additional contributions from excitations into the LUMO+1. LUMO and LUMO+1 in the core-excited naphthalene are separated by >1 eV.[28] However, the transition into the LUMO+1 is calculated to have very low intensity due to small overlap of the LUMO+1 with the 1*s* orbital of the excited atomic site. This in turn leads to quite small values for the oscillator strength of the $1s \rightarrow$LUMO+1 transition. Therefore, the observed profile of the π_2^* peaks is most likely not influenced by excitations into the LUMO+1. Another possible explanation is that the last vibrational feature from the π_1^* band overlaps with the π_2^* and produces a double structure (Fig. 5).

In the NEXAFS simulations we consider all vibrational modes of the naphthalene molecule. The vibrational splitting for the three atomic sites originates predominantly from two or three modes (Table V, VI, and VII). All vibrational modes (with one exception—mode 41, at site C2) are excited only up to the second vibrational level. This indicates that the potential surface of the excited state is only slightly displaced from that of the ground state. This is very different from the case of (small) linear molecules, like ethylene,[21] and might be a consequence of the rigidity of more two-dimensional systems. Compared to one-dimensional structures,[36] the polaronic distortion accompanying charges in two-dimensional systems is smaller.[9,10] Nevertheless, this small displacement is sufficient to create visible vibrational fine structure in the NEXAFS spectrum of naphthalene.

The main contribution in the vibrational structure is due to C-C stretching modes (Fig. 6 and Tables V, VI, VII). Most of the C-H modes show substantial gradients of the PS, however, their contribution to the vibrational splitting is quite small. Two main reasons for this behavior can be pinpointed.

(i) First, the LUMO of naphthalene almost does not contain contributions from the hydrogen 1*s* orbitals. This implies small changes of the electronic potential in the vicinity of the hydrogen atoms upon core-excitation at carbon atoms and, consequently, only minor contributions from C-H modes.

(ii) The FC amplitude [given in Eq. (3)] is strongly dependent on the vibrational frequency [Eq. (2)], and hence,

TABLE VI. Franck-Condon factors for the strongest vibrational modes in the core excitation at the C2 site—NEXAFS.

Mode	ω (eV)	Symmetry	FC factors $\langle 0\|0\rangle^2$	$\langle 0\|1\rangle^2$	$\langle 0\|2\rangle^2$
11	0.210	A_g	0.924	0.073	0.003
12	0.205	B_{3u}	0.943	0.055	0.002
18	0.169	B_{2u}	0.975	0.024	0.000
19	0.167	B_{1g}	0.856	0.133	0.010
30	0.125	B_{3u}	0.940	0.058	0.002
38	0.099	A_g	0.794	0.183	0.021
41	0.068	B_{1u}	0.460	0.357	0.138

higher frequency causes the FC factors to increase and quenches the vibrational fine structure. As the C-H stretching modes have usually higher vibrational frequencies than the C-C modes, the effect of high gradients is diminished.

As mentioned above, feature π_1^* contains overlapping contributions from C2 and C3 excitations. In this case, the observation of a clearly resolved vibrational splitting in the π_1^* feature can only be explained if the chemical shift between these two sites matches the vibrational energy of about 170 eV. In the simulations, a chemical shift of about 200 meV is obtained, leading to a different profile in the onset region of the π_1^* resonance, and even displaying two vibrational peaks. A better agreement with the experiment is achieved when the C2 peak is artificially moved towards the C3 peak by about 100 meV (Fig. 7).

All aforementioned calculations have been performed at the ΔDFT level using the DEMON code. Within this method, an open-shell system is treated by an unrestricted formalism. In the current implementation, an unrestricted calculation produces a spin-contaminated state, that is, a state with small contributions from triplet states. This introduces an error on the level of the exchange integral between the 1*s* and the electron excited into the LUMO, which could be responsible for the discrepancy between theory and experiment. The exchange integral $\langle 1s,\mathrm{LUMO}|\mathrm{LUMO},1s\rangle$ is estimated to be about 0.2 eV.

In order to avoid spin-contamination, the correct singlet state needs to be constructed. For that purpose, we tested two different methods for computating core-hole excitation energies. These methods include the restricted open-shell Hartree-Fock (ROHF) technique in the program package DALTON[32] and the generalized valence bond method (GVB) in GAMESS-US.[37]

As expected, ROHF performs poorly. Although it provides values close to the correct excitation energies for the C2 and C3 sites, the calculation seems to be inaccurate because the core orbitals are described as delocalized states. It is known[21] that a localized description of the core hole is needed to account for important relaxation effects. For the second method, using the GAMESS-US package, a Boys localization procedure and a GVB calculation were employed. The energy difference between C2 and C3 is again about 200 meV (Table VIII), similar to the ΔDFT calculation. Constructing the correct spin state does not improve the chemical shift between the C2 and C3 sites in the NEXAFS spectrum.

With a total margin of error of 100–200 meV, the present accuracy of *ab initio* methods used for the calculation of relative electronic transition energies from core levels is too coarse to reproduce these small effects.

TABLE VII. Franck-Condon factors for the strongest vibrational modes in the core excitation at the C3 site—NEXAFS.

Mode	ω (eV)	Symmetry	FC factors $\langle 0\|0\rangle^2$	$\langle 0\|1\rangle^2$	$\langle 0\|2\rangle^2$
9	0.220	B_{1g}	0.837	0.149	0.013
10	0.214	B_{2u}	0.966	0.033	0.001
11	0.210	A_g	0.987	0.013	0.000
18	0.169	B_{2u}	0.983	0.017	0.000
19	0.167	B_{1g}	0.900	0.095	0.005
31	0.121	B_{1g}	0.924	0.073	0.003
35	0.105	B_{2g}	0.872	0.119	0.008

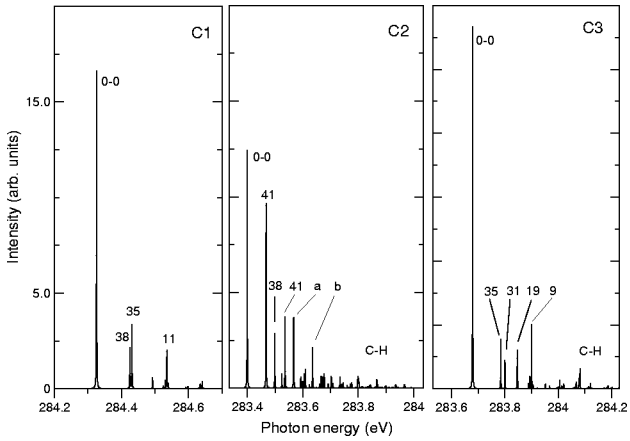

FIG. 6. Spectral lines of the NEXAFS for the three atomic sites, without life-time broadening. (a) Denotes three overlapping peaks—(0→1) transition for modes 18, 19, and a double (0→1) excitation of modes 38 and 41. (b) Denotes a double (0→1) excitation of modes 18 and 41.

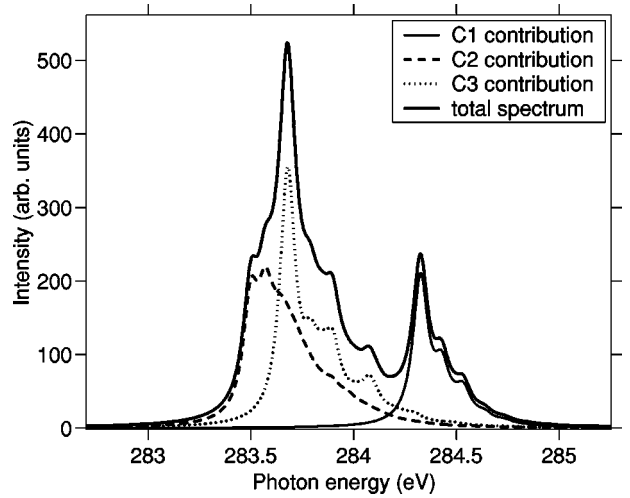

FIG. 7. Calculated NEXAFS spectrum of naphathalene and the contributions from the three chemically different atomic sites, with the absorption energy for the C3 site being artificially lowered by 0.1 eV.

TABLE VIII. Excitation energies (in eV) and oscillator strengths ($f_{\Delta DFT}$) of the three distinguishable carbon atoms in naphthalene using ROHF in DALTON, GVB in GAMESS-US, and ΔDFT in DEMON.

		C1	C2	C3
$1s \rightarrow$LUMO	ω_{ROHF}	291.079	296.653	296.693
	ω_{GVB}	286.986	285.955	286.141
	$\omega_{\Delta DFT}$	284.397	283.583	283.814
	$f_{\Delta DFT}$	0.0162	0.0270	0.0252

VI. CONCLUSIONS

The fine structure of C(1*s*) photoionized and core-excited states at the three chemically different carbon atomic sites of the free naphthalene molecule has been experimentally resolved and theoretically analyzed. Although the high experimental resolution still represents a challenge to the calculation of absolute electronic transition energies from core levels, the spectral profile is well reproduced allowing an asignment of individual features in the fine structure of the spectra.

Compared to linear systems, the rigidity of the two-dimensional lattice of the naphthalene molecule is responsible for only a rather small geometrical relaxation in the neutral core-excited or ionic final states, as manifested in the small displacement of the potential surfaces, the vibrational broadening of the photoelectron emission lines, and x-ray absorption resonances.

The vibrational fine structure is dominated by particular C-C stretching modes, and in the case of XPS of the C2 and C3 sites also by high-energy C-H stretching modes. The suppression of certain modes is found to be, to a great extent, caused by the increase of the FC factors due to the high frequencies of these modes. Since features arising from C-H stretching modes are virtually absent in the naphthalene valence spectrum, a strong dependence of the charge-vibrational coupling on the electronic density distribution in the individual orbitals is observed.

When it is possible to separate chemical shifts and vibrational excitations in such medium-size molecules, larger and more complex systems can and will be addressed in the near future with the same level of accuracy. Importantly, the improved knowledge of electronic and vibronic relaxation phenomena in molecules will provide an understanding of optical and transport phenomena in molecular materials.

ACKNOWLEDGMENTS

The authors thank M. Tchaplyguine (Uppsala University, Sweden) for technical assistance, L. Saethre (University of Bergen, Norway), and V. Coropceanu (Georgia Institute of Technology, Atlanta, USA) for fruitful discussions. The work is performed in a collaboration within the Center for Advanced Molecular Materials (CAMM), funded by the Swedish Science Foundation (SSF) and additionally supported by the Swedish Research Council (VR) under Contract Nos. 12252003 and 12252020. In addition, research in Linköping is supported by a Research Training Network (LAMINATE, Project No. 00135) and the EU-Growth project MAC-MES (Project No. GRD-2000-30242).

[1] Y. Ma, F. Sette, G. Meigs, S. Modesti, and C. T. Chen, Phys. Rev. Lett. **63**, 2044 (1989).
[2] M. Neeb, B. Kempgens, A. Kivimäki *et al.*, J. Electron Spectrosc. Relat. Phenom. **88**, 19 (1998).
[3] P. Skytt, P. Glans, J.-H. Guo *et al.*, Phys. Rev. Lett. **77**, 5035 (1996).
[4] V. Myrseth, K. A. Børve, K. Wiesner, M. Bässler, S. Svensson, and L. Sæthre, Phys. Chem. Chem. Phys. **4**, 5937 (2002).
[5] U. Hoefer, M. J. Breitschafter, and E. Umbach, Phys. Rev. Lett. **64**, 3050 (1990).
[6] S. Kera, H. Yamane, I. Sakuragi, K. K. Okudaira, and N. Ueno, Chem. Phys. Lett. **364**, 937 (2002).
[7] J. Bozek, T. X. Carrol, J. Hahne, L. J. Saethre, J. True, and T. D. Thomas, Phys. Rev. A **57**, 157 (1998).
[8] F. Burmeister, S. L. Sorensen, O. Björneholm *et al.*, Phys. Rev. A **65**, 012704 (2002).
[9] V. Coropceanu, M. Malagoli, D. A. da Dilva Filho, N. E. Gruhn, T. G. Bill, and J. L. Brédas, Phys. Rev. Lett. **89**, 275503 (2002).
[10] D. A. da Silva Filho, R. Friedlein, V. Coropceanu *et al.*, Chem. Comm (in press).
[11] R. Feifel, F. Burmeister, P. Salek *et al.*, Phys. Rev. Lett. **85**, 3133 (2000).
[12] A. B. Preobrajenski, A. S. Vinogradov, S. L. Molodtsov, S. K. Krasnikov, T. Chassé, R. Szargan, and C. Laubschatt, Phys. Rev. B **65**, 205116 (2003).
[13] R. Friedlein, S. L. Sorensen, A. Baev *et al.*, Phys. Rev. B **69**, 125204 (2004).
[14] P. A. Brühwiler, O. Karis, and N. Mårtensson, Rev. Mod. Phys. **74**, 703 (2002).
[15] F. Gel'mukhanov and H. Ågren, Phys. Rev. B **57**, 2780 (1998).
[16] T. Privalov, F. Gel'mukhanov, and H. Ågren, Phys. Rev. B **59**, 9243 (1999).
[17] Y. Luo, H. Ågren, J. Guo, P. Skytt, N. Wassdahl, and J. Hordgren, Phys. Rev. A **52**, 3730 (1995).
[18] W. Osikowicz, R. Friedlein, M. P. de Jong, S. L. Sorensen, L. Groenendaal, and W. R. Salaneck (unpublished).
[19] J. Stöhr, NEXAFS *Spectroscopy*, Springer Series in Surface Science, Vol. 25 (Springer, Berlin, 1992).
[20] F. Gel'mukhanov and H. Ågren, Phys. Rev. A **49**, 4378 (1994).
[21] H. Köppel, F. X. Gadea, G. Klatt, J. Schirmer, and L. S. Cederbaum, J. Chem. Phys. **106**, 4415 (1997).
[22] W. E. Egelhoff, Jr., in *Core-level Binding-energy Shifts at Surfaces and Solids*, Surface Science Reports: a Review Journal, Vol. 6 (North-Holland, Amsterdam, 1987).
[23] W. Domcke and L. Cederbaum, Chem. Phys. **25**, 189 (1977).
[24] M. Bässler, J.-O. Forsell, O. Björneholm *et al.*, J. Electron Spectrosc. Relat. Phenom. **101**, 953 (1999).
[25] U. Hergenhahn, J. Phys. B **37**, R89 (2004).
[26] C. Kolczewski, R. Püttner, O. Plashkevych *et al.*, J. Chem. Phys. **114**, 6426 (2001).
[27] V. Caravetta, O. Plashkevych, and H. Ågren, Chem. Phys. **263**, 231 (2001).
[28] H. Ågren, O. Vahtras, and V. Caravetta, Chem. Phys. **196**, 47 (1995).
[29] O. Plashkevych, T. Privalov, H. Ågren, V. Caravetta, and K. Ruud, Chem. Phys. **260**, 11 (2000).
[30] V. Caravetta, O. Plashkevych, and H. Ågren, J. Chem. Phys. **109**, 1456 (1998).
[31] M. J. Frisch, G. W. Trucks, H. B. Schlegel *et al.*, GAUSSIAN 03, Revision B.03, Gaussian, Inc., Pittsburgh, PA, 2003.
[32] T. Helgaker, H. J. Aa. Jensen, P. Jorgensen *et al.*, DALTON a molecular electronic structure program, Release 1.2 (2001).
[33] M. E. Casida, C. Daul, A. Goursot *et al.*, DEMON-KS version 4.0.
[34] L. Triguero, L. G. M. Petersson, and H. Ågren, Phys. Rev. B **58**, 8097 (1998).
[35] A. P. Hitchcock, M. Pocock, C. E. Brion, M. S. Banna, D. C. Frost, C. A. MacDowell, and B. Wall-bank, J. Electron Spectrosc. Relat. Phenom. **13**, 345 (1978).
[36] W. R. Salaneck, R. H. Friend, and J. L. Brédas, Phys. Rep. **319**, 231 (1999).
[37] M. W. Schmidt, K. K. Baldridge, J. A. Boatz *et al.*, J. Comput. Chem. **14**, 1347 (1993).